A New Approach to High Efficincy in Isolated Boost Converters for High-Power Low-Voltage Fuel Cell Apllications

Nymand, Morten; Andersen, Michael A. E.

Published in:
13th Power Electronics and Motion Control Conference

Link to article, DOI:
10.1109/EPEPEMC.2008.4635255

Publication date:
2008

Document Version
Peer reviewed version

A New Approach to High Efficiency in Isolated Boost Converters for High-Power Low-Voltage Fuel Cell Applications

Morten Nymand*, Michael A.E. Andersen†

* University of Southern Denmark/Dept. of Sensors, Signals and Electrotechnics, Odense, Denmark, *mny@sense.sdu.dk*

† Technical University of Denmark/Dept. of Electrical Engineering, Lyngby, Denmark, *ma@elektro.dtu.dk*

***Abstract*—A new low-leakage-inductance low-resistance design approach to low-voltage high-power isolated boost converters is presented. Very low levels of parasitic circuit inductances are achieved by optimizing transformer design and circuit lay-out. Primary side voltage clamp circuits can be eliminated by the use of power MOSFETs fully rated for repetitive avalanche. Voltage rating of primary switches can now be reduced, significantly reducing switch on-state losses. Finally, silicon carbide rectifying diodes allow fast diode turn-off, further reducing losses. Test results from a 1.5 kW full-bridge boost converter verify theoretical analysis and demonstrate very high efficiency. Worst case efficiency, at minimum input voltage maximum power, is 96.8 percent and maximum efficiency reaches 98 percent.**

***Keywords*—Switched-mode power supply, fuel cell system, efficiency, transformer, SiC-device.**

I. INTRODUCTION

High-power fuel cell or battery powered applications such as for transportation, forklift trucks or distributed generation, are often faced with the need for boosting the low input voltage (30-60V) to the much higher voltage (360-400V) required for interfacing to the utility grid fig. 1, [1].

For safety as well as for EMC reasons, galvanic isolation between source and utility grid is often desirable or required.

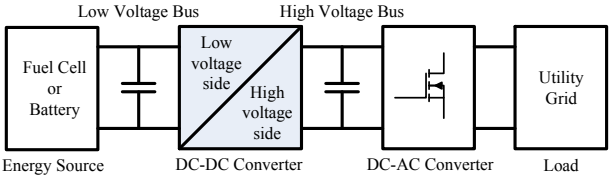

Fig.1. Fuel cell power system with isolated high gain DC-DC converter.

In particular fuel cells, exhibit significant output impedance reducing output voltage as output power is increased. System peak power is therefore reached at converter minimum input voltage. Drop in converter efficiency at minimum input voltage and maximum output power therefore directly reduces available system peak power. While the converter is required to operate over a wide input voltage range, typically up to a factor 1:2, high converter efficiency becomes particular important at minimum input voltage maximum power [1].

Isolated boost converters has some inherent advantages when used in fuel cell applications. With the storage inductor placed at the input side, ripple current is inherently low, only requiring limited extra filtering at the input side.

Output rectifying diodes are placed directly across output capacitors, ensuring minimum voltage stress and effective voltage clamping.

In a 400 V output application, 600 V rated diodes will be sufficient in boost type topologies, whereas buck type topologies would require 1200 V diodes or stacking of multiple outputs. Voltage stress on boost topology diodes are thus less than half of the corresponding voltage stress on a buck derived topology. Buck type topologies will therefore have significantly larger rectifying losses than boost type topologies.

The draw back of the boost type topologies is the need for clamping voltage spikes on primary switches caused by transformer leakage inductance and parasitic circuit inductances. Clamping is typically performed by some sort of voltage clamp circuit or by implementing active reset circuits [2-7]. This however requires significantly increased voltage rating on primary switches severely penalising conduction losses.

A large number of isolated boost converters for fuel cell applications have been presented, among these [2-7]. Ref. [2-4] have input voltage range and power level that are comparable to the converter presented in this paper. Ref. [5-7] are isolated bi-directional full-bridge boost converters intended for electrical vehicles. Input voltage is 12 V (8-15V), output voltage is typically 250-420 V and power range, in boost mode, is from 1.5 kW [5,6] to 3 kW [7].

Even though vastly different designs are represented (hard switched push-pull boost [2], actively clamped, two-inductor boost [3], bi-directional, actively clamped, two-inductor boost [4], and bi-directional soft switching full-bridge boost converters [5-7]), a general efficiency trend is clear. All converters achieve high efficiencies in the medium to high input voltage range, typically peaking at 94-96 percent at medium power. At low input voltage, high power, efficiency however reduces significantly to approx. 90 percent or below.

In this paper, the design of a simple, wide input voltage range, isolated full-bridge boost converter with very high efficiency at low input voltage is presented.

Test results from a 1.5 kW demonstration model achieve peak efficiency of 98 percent. Worst case

efficiency at minimum input voltage and maximum power is 96.8 percent.

II. ISOLATED FULL-BRIDGE BOOST CONVERTER

The proposed full-bridge boost converter is presented in fig. 2. Timing diagrams and basic operating waveforms are presented in fig. 3.

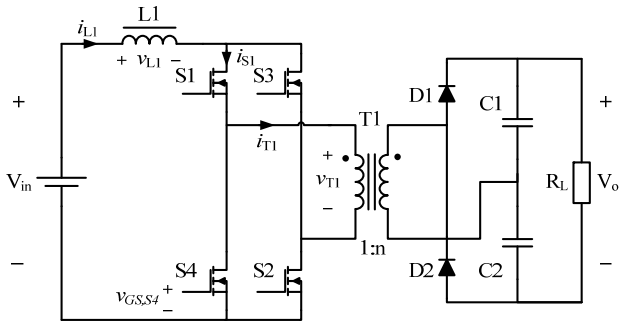

Fig.2. Isolated full-bridge boost converter with voltage doubling rectifier.

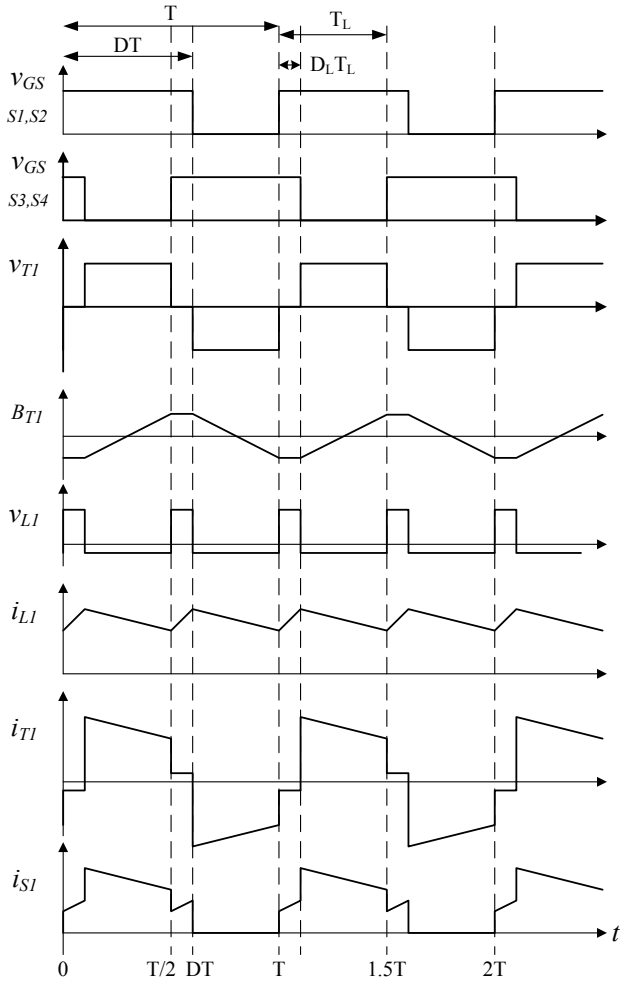

Fig.3. Basic operating waveforms of isolated full-bridge boost converter.

A. Basic converter operation

Primary switches S1-S4, are hard switched and operated in pairs S1-S2, and S3-S4, respectively. Drive signals are 180 degrees phase shifted. Switch transistor duty cycle D, is above 50 percent to ensure switch overlap and thus a continuous current path for the inductor L1, current.

Energy transfer to output starts when switches S3 and S4 are turned off. Inductor current i_{L1}, flows through primary switch S1, transformer T1, rectifier diode D1, output capacitor C1 and returns to input through primary switch S2. Inductor current i_{L1}, discharges. The period ends when primary switches S3 and S4 are turned on again.

During switch overlap, when all switches S1-S4, are turned on, inductor current $i_{L1,}$ is charged. Current in the transformer secondary winding is zero and diodes D1 & D2 are off. Transformer magnetizing current circulates in the transformer primary winding through switches S2-S4 and/or S1-S3. Capacitors C1, C2, supply the load current. The period ends when primary switches S1and S2 are turned off.

A second energy transfer cycle starts when switches S1 and S2, are turned off and ends when S1 and S2 are turned on again. Inductor current $i_{L1,}$ flows through switches S3, T1, D2, C2, and returns to input through S4.

Finally, a second inductor charging interval similar to the first follows.

The converter transfer function in continuous steady state is:

$$\frac{V_o}{V_{in}} = \frac{n}{1-D} \tag{1}$$

Where n=Ns/Np is the transformer turns ratio, and D is the switch duty cycle (0.5≤ D<1).

The corresponding inductor duty cycle D_L, and period time T_L, is defined as:

$$D_L \equiv 2D\text{-}1 \tag{2}$$

$$T_L \equiv {}^{T}/_{2} \tag{3}$$

Where $T=1/f_S$ is the period time for switches, diodes and the transformer.

III. CONVERTER DESIGN

The four primary switches S1-S4, are 75 V, 2.8 mΩ International Rectifier IRFB 3077 Power MOSFET which are fully repetitive avalanche rated [8]. The two rectifier diodes D1-D2, are 600 V Infineon IDT 10S60C SiC Schottky diodes. The inductor L1, core is a Magnetics Kool Mμ 77439. The transformer core is an EE55/21 ferrite core in 3F3 material. Switching frequency is 45 kHz.

Low current switching times increase efficiency since less charge is being diverted from output into primary side clamp circuits. Current switching times are limited by transformer leakage inductance and primary side stray inductances as well as MOSFET common source inductance whichever is worst case [9].

Transformer leakage inductance can be reduced by extensive interleaving of primary and secondary windings.

Careful primary side lay-out is required to reduce primary side stray inductances. MOSFET common source inductance is a function of package internal wiring (bonding wire length) as well as source external lead length [9].

B. Transformer design

The low input voltage, high power in fuel cell converters, causes high currents to flow in transformer primary windings requiring large copper cross sections in primary windings.

Foil windings are very efficient in providing large copper cross sections with a minimum conductor thickness. However, as power levels increases, even foil winding thicknesses quickly approach or exceed penetration depths in copper. Proximity effect can thereby cause very significant increases in winding AC resistances and thus lead to significantly increased power losses [10,11].

At 45 kHz, penetration depth in copper is only 0.34 mm. A primary winding with 4 turns on an EE55/21 core would allow up to approximately 0.6 mm cobber thickness for each of the 4 primary turns. Winding these 4 turns in a single 4 layer section, would increase AC resistance approximately 13 times compared to winding DC resistance ($F_R=R_{AC}/R_{DC}=13$) [10,11].

The more frequent case of a single interleaving (primary winding interleaved between two sections of secondary windings), increases AC resistance by a factor 3.5 compared to winding DC resistance.

To avoid severe proximity effect, penetration from both sides of each primary turn can be obtained by interleaving each primary turn between sections of secondary windings. The corresponding increase in AC resistance is now only 5 percent ($F_R=1.05$).

Keeping AC resistances low in high frequency high-current transformers therefore requires extensive interleaving of windings.

Since interleaving of windings also has the well known effect of reducing transformer leakage inductance [snelling], these transformers will not only have small AC resistances but also extremely low leakage inductances.

AC resistance and leakage inductance of the transformer used in a 1.5 kW isolated boost converter with a turn ratio of 4, are presented in fig. 4. Transferred to primary side, the AC resistance is only 1.9 mΩ and leakage inductance is only 11 nH. The leakage inductance in percent of primary inductance is only 0.01 percent.

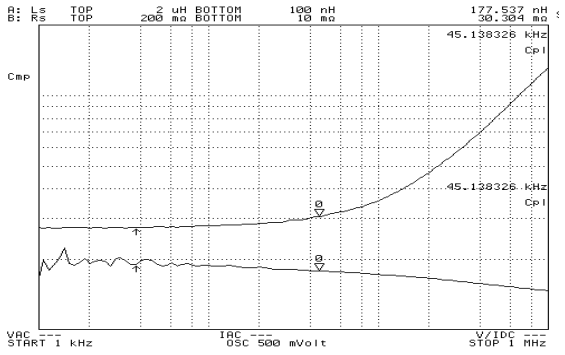

Fig.4. Measured secondary side AC resistance (upper curve) and leakage inductance (lower curve) of 1.5 kW transformer.

C. Primary switch voltage clamping

At low input voltage and high power levels, conduction losses in primary switches are a dominant loss factor. In the voltage range 60-200V, MOSFET on-resistance $R_{DS,ON,}$ typically increases quadratic with increasing drain-to-source breakdown voltage $V_{(BR)DSS}$. Voltage rating of primary switches therefore has very significant impact on converter conduction loss and thereby on converter efficiency.

To allow clamp circuits to clamp voltage spikes caused by transformer leakage inductance and circuit stray inductances, voltage rating of primary switches, in isolated boost converters, is typically rated at 2-3 times the maximum input voltage [6].

For primary clamp circuits to be effective, they need to present significantly lower impedance at the clamping point than the circuit which is being clamped. However, with the very low levels of transformer leakage inductances that are achieved in low voltage high power transformers, it becomes indeed very difficult for clamp circuits to present lower impedances than that of the transformer itself.

This result in clamp circuits only taking (small) fractions of the clamp energy, since the major part is being clamped by the transformer which even has lower reflected voltage and thus higher driving voltage across the leakage inductance.

Fortunately, due to the very low leakage inductance in the transformer, the leakage energy in the transformer is very small.

Some new low voltage power MOSFETs are rated for repetitive avalanche and are very robust to unclamped inductive switching [8,12].

With careful primary side lay-out and low leakage design of transformers, converter leakage energy is very small. Using avalanche rated MOSFETs, primary side clamp circuits can be eliminated and switch voltage rating reduced, significantly reducing MOSFET conduction losses.

Since silicon carbide Schottky diodes do not suffer from reverse recovery, they can work at much higher switching frequencies and in particular at much faster current switching speed (turn-off di/dt) without excessive losses.

IV. EXPERIMENTAL RESULTS

Experimental results from 1.5 kW demonstration model are presented in the following.

Fig. 4, is a plot of transformer leakage inductance and AC-resistance measured on secondary side. Transferred to primary side (dividing by transformer turns-ratio squared), the transformer leakage inductance is only 11 nH and the AC-resistance at 45 kHz is only 1.9 mΩ.

Fig. 5, is a plot of voltages and currents in the converter. Transformer current is measured on secondary side in order to avoid adding extensive stray inductance to the primary circuit.

Fig. 6, is an expanded view of fig. 5, showing that at turn off output current rise is only delayed approximately 30 ns from transistor voltage rise. Total avalanche loss, shared between 4 primary switches, can be estimated to:

$$P_{Aval,S1-S4} \approx i_{L1,peak} v_{S1,av} \Delta t f_s = 3.75\ W \qquad (4)$$

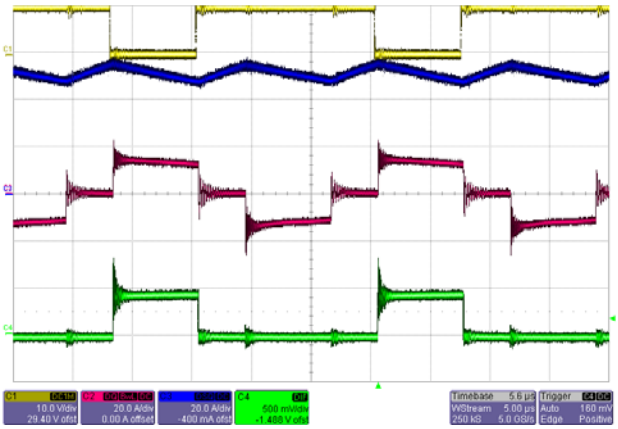

Fig.5. Measured converter waveforms at 30V input and 1.5 kW output power. From top: control signal for transistor S4, inductor L1 current (20A/div), transformer secondary current (20A/div) and bottom trace is transistor S4 drain-source voltage (50V/div). Time base is 5µs/div.

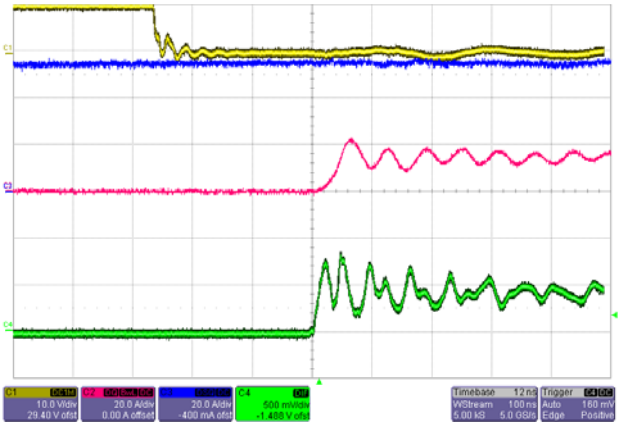

Fig. 6. Expanded view of fig. 5. Time base is 100ns/div.

D. Efficiency measurement

Measuring efficiencies in the 97-98 percent range are particularly critical and extensive care has been taken to ensure very high precision and stability of the efficiency test set-up.

In particular the current measurements are very critical. Measurements were made using 0.1 percent sense resistors with very high temperature stability (<10 ppm) mounted on heat sinks. Sense cables were shielded and supplied with common mode attenuating coils. Agilent 34410A high precision multimeters were used.

Since efficiency of single-input, single-output DC-DC converters is equal to the product of voltage ratio and current ratio (2), the critical current measurement ratio can be checked by simply passing the same current through both current sensors in series and verify that the measured voltage ratios correspond to the ratio of the sense resistor resistances.

$$\eta = \frac{V_o}{V_{in}} \frac{I_o}{I_{in}} \qquad (5)$$

Stability of test set-up was furthermore ensured by using high stability power sources and electronic loads. Converter heat sink temperature was measured and limited to 40 degree Celsius for repeatability of test.

The measured deviation of the sense resistor voltage ratio compared with the specified ratio (measured at 10 amperes) was less than 0.01 percent.

According to the specification of the Agilent 34410A, the output/input voltage ratio can be measured with a precision of better than +/- 0.012 percent.

The combined precision of the efficiency measurements are better than +/- 0.1 percent.

Measured converter efficiency, including transistor drive losses, is presented in fig. 7.

Maximum efficiency at low input voltage is 97.5 percent. Efficiency at full load is between 96.8 and 97.9 percent. Maximum efficiency is 98 percent.

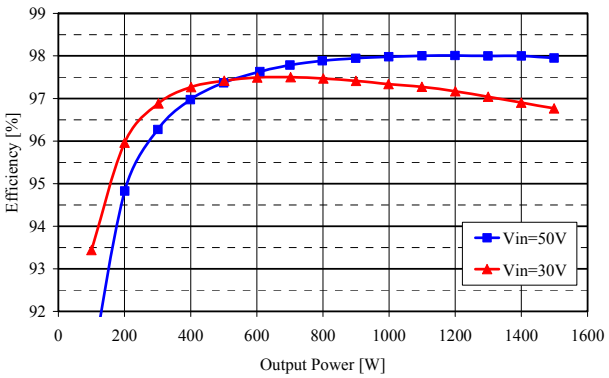

Fig. 7. Converter efficiency including drive power.

A detailed break down of converter power loss at minimum input voltage, maximum power (30 V/1.5 kW), is presented in table 1.

As would be expected, losses are dominated by conduction losses which constitute 83 percent of all calculated losses. Notice also that even though hard switching is used, switching losses are very small. Total inductive clamp losses are only 3.75 W corresponding to a quarter of a percent loss of efficiency.

Transformer efficiency is above 99.6 percent at maximum power.

TABLE I.
CONVERTER POWER LOSS BREAK DOWN AT 1.5 KW / 30 V

Component	Loss type	Loss [W]	Total [W]
MOSFET	Conductive	14.1	18.8
	Capacitive	0.27	
	Drive	0.72	
	Inductive clamp	3.75	
Diodes	Conductive	14.7	15.1
	Capacitive	0.41	
Transformer	Conductive	3.77	5.5
	Core	1.75	
Inductor	Conductive	5.2	6.2
	Core	1.0	
Other	Misc.		4.5
Converter	Measured efficiency		50.1

A photo of the 1.5 kW demonstration model is shown in fig. 8.

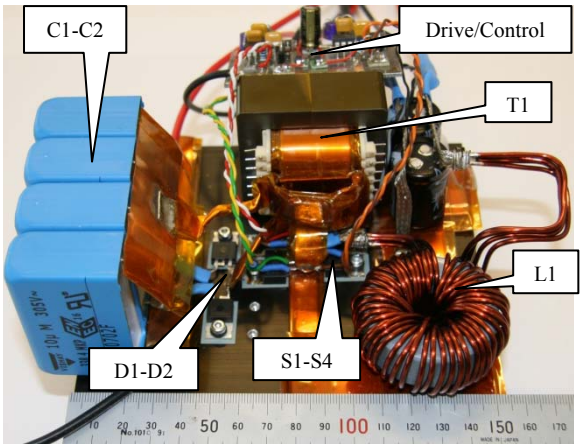

Fig. 7. Photo of 1.5 kW isolated full-bridge boost converter.

V. Conclusion

This paper, has presented a design approach to achieve very high efficiency in low-voltage, high-power, isolated boost converters. The design approach is demonstrated on an isolated full-bridge boost converter. Converter operation has been analysed and design details for a 1.5 kW converter has been presented.

Fast current switching is achieved by careful design of transformer and converter layout. Transformer proximity effect losses are reduced by extensive interleaving of primary and secondary windings. Test results on a 1.5 kW demonstration model confirm the achievement of fast current switching, low parasitic circuit inductance and very high efficiency.

Worst case efficiency, at maximum load and minimum input voltage, is 96.8 percent. Maximum efficiency is 98 percent.

References

[1] F. Profumo, A Tenconi, M. Cerchio, R. Bojoi, G. Gianolio, ''Fuel cells for electric power generation: Peculiarities and dedicated solutions for power electronic conditioning systems'', *EPE Journal* vol. 16, no. 1 February 2006, pp. 44-50.

[2] G. K. Andersen, C. Klumpner, S. Kjær, F. Blaabjerg, ''A new power converter for fuel cells with high system efficiency'', *International Journal of Electronics*, 2003, vol. 90, pp. 737-750.

[3] J. T. Kim, B. K. Lee, T. W. Lee, S. J. Jang, S. S. Kim, C. Y. Won, ''An active clamping current-fed half-bridge converter for fuel-cell generation systems'', *Conf. Proc. IEEE PESC 2004*, Aachen, Germany, pp. 4709-4714.

[4] H. Xiao, L. Guo, S. Xie, ''A new ZVS bidirectional DC-DC converter with phase-shift plus PWM control scheme'', *Conf. Proc. IEEE APEC 2007*, pp. 943-948.

[5] K. Wang, C.Y. Lin, L. Zhu, D. Qu, F.C. Lee, J.S. Lai, ''Bi-directional DC to DC converter for fuel cell systems'', *Conf. Proc. IEEE Power Electronics in Transportation 1998*, pp. 47-51.

[6] K. Wang, L. Zhu, D. Qu, H. Odendaal, J. Lai, F.C. Lee, ''Design, implementation, and experimental results of bi-directional full-bridge DC/DC converter with unified soft-switching scheme and soft-starting capability'', *Conf. Proc. IEEE PESC 2000*, pp. 1058-1063.

[7] L. Zhu, ''A novel soft-commutating isolated boost full-bridge ZVS-PWM DC-DC converter for bidirectional high power applications'', *IEEE Transactions on Power Electronics*, vol. 21, no. 2, March 2006, pp. 422-429.

[8] International Rectifier IRFB3077 Datasheet PD-97047A, 020806.

[9] S. Havanur, ''Quasi-clamped inductive switching behaviour of power MOSFETs'', *Conf. Proc. IEEE PESC 2008,* Rhodes, Greece, pp. 4349-4354.

[10] P. L. Dowell, ''Effects of eddy currents in transformer windings'', *Proc. IEE,* vol. 113, no. 8, August 1966, pp. 1387-1394.

[11] E. C. Snelling, *Soft Ferrites – Properties and Applications.* Butterworths, 2nd. Ed., 1988.

[12] T. McDonald, M. Soldano, A. Murray, T. Avram, ''Power MOSFET avalanche design guidelines'', *Application note AN-1005,* International Rectifier.